Investigation of the Rayleigh-Taylor and Richtmyer-Meshkov instabilities

Research Funded under the
Stewardship Science Academic Alliances Program

DOE Grant ID Number: DE-FG52-03NA00061

Riccardo Bonazza, Mark Anderson and Leslie Smith

Department of Engineering Physics
University of Wisconsin - Madison

Technical report for the period September 2003-September 2004

1 Introduction

The present research program is centered on the experimental and numerical study of two instabilities that develop at the interface between two different fluids when the interface experiences an impulsive or a constant acceleration. The instabilities, called the Richtmyer-Meshkov and Rayleigh-Taylor instability, respectively, adversely affect target implosion in experiments aimed at the achievement of nuclear fusion by inertial confinement by causing the nuclear fuel contained in a target and the shell material to mix, leading to contamination of the fuel, yield reduction or no ignition at all.

2 Accomplishments

2.1 Richtmyer-Meshkov instability (spherical interface)

The RM experiments are performed in a vertical shock tube of large, square internal cross section. The shock tube is about 9 m long, with a 1.8 m driver section. A shock wave is generated by rupturing a steel diaphragm by gas overpressure. The driver section is at the top of the facility hence the shock initially travels downwards.

All RM shock tube experiments involve:
1) preparation of a gas interface;
2) acceleration of the interface by a shock wave;
3) measurement of relevant quantities at the interface, usually by optical diagnostics.

During the first year of funding (11/2002-11/2003) our efforts had focused on the generation of a suitable interface to subject to shock acceleration. For a shock tube experiment to be of scientific value, generation of the interface must be a well controlled, repeatable process and the interface geometry (the experiment's initial conditions) must be known in detail. An ideal interface is two-dimensional, massless, infinitely sharp (no diffusion across it), with a known modal composition but such interface is not readily attainable in a laboratory. In the present year, we have completed the

development of two different interfaces, with several of the properties listed above: an axisymmetric, nearly spherical, soap film interface (a bubble); and a massless, diffuse, 2-D, single-mode interface.

2.1.1 Laboratory Experiments

The bubble interface is produced inside the shock tube by placing a known quantity of soap film at the tip of an injector initially protruding from the shock tube wall, blowing the bubble, forcing the bubble to detach from the injector and retracting the injector into the shock tube wall. This leads to a free-falling bubble and to minimal disruption of the incoming shock wave by the non perfectly flat shock tube wall at the location where the injector is retracted. This setup is a significant improvement over that described in last year's report, and used for some preliminary tests, where the injector was fixed and protruded inside the shock tube. The new setup is schematically shown in Fig.1.

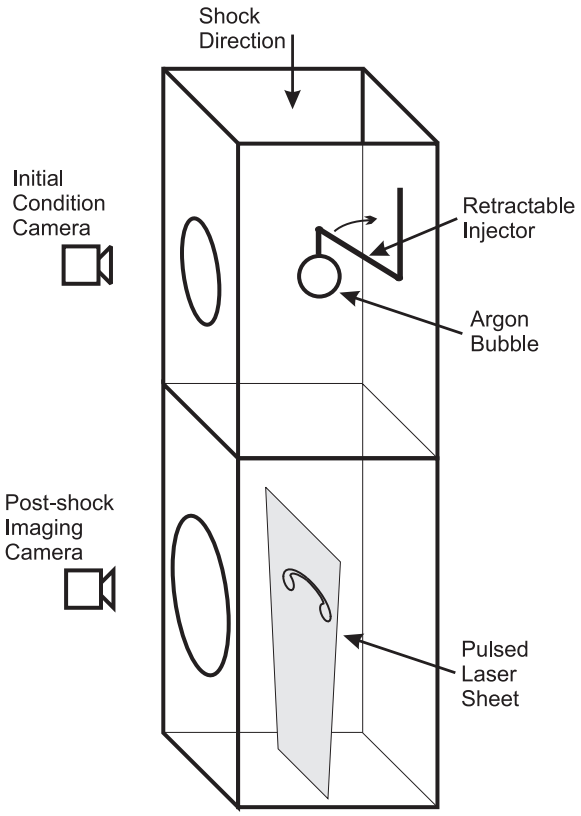

Figure 1: Schematic of retractable injector.

Very extensive shock tube experiments have been performed with the free-falling bubble. The experimental setup used to visualize the bubble during its free fall and after interaction with the incoming shock is also shown in Fig.1. The bubble is imaged during formation and during the initial stages of its free fall using continuous, white, front lighting and a medium resolution (512 $\times$ 512 pixel) medium framing rate (260 fps) CCD camera. The bubble is subsequently imaged at two different time delays after shock acceleration, using planar imaging performed with an Nd:YAG laser (at 532 nm) and a single, high resolution (1024$\times$ 1024 pixels) scientific grade CCD camera.

The experiments are performed in full darkness so that the two laser pulses generate two separate images on a single CCD sensor. The laser light is scattered from the shocked bubble towards the CCD sensor by the soap film which atomizes upon shock acceleration and thereafter acts as a suitable flow-tracer, making this a planar Mie scattering visualization technique.

All experiments are performed with the shock tube's driven section initially at atmospheric pressure and room temperature. The driver, driven and test gases are always helium, nitrogen and argon, respectively, yielding an Atwood number at the argon/nitrogen interface of $A = (\rho_{Ar} - \rho_{N2})/(\rho_{Ar} + \rho_{N2})$=0.18. Shock strengths of $M = 1.3$, $M = 2.88$ and $M = 3.38$ have been used. A typical time series of shocked bubble images is presented in Fig.2

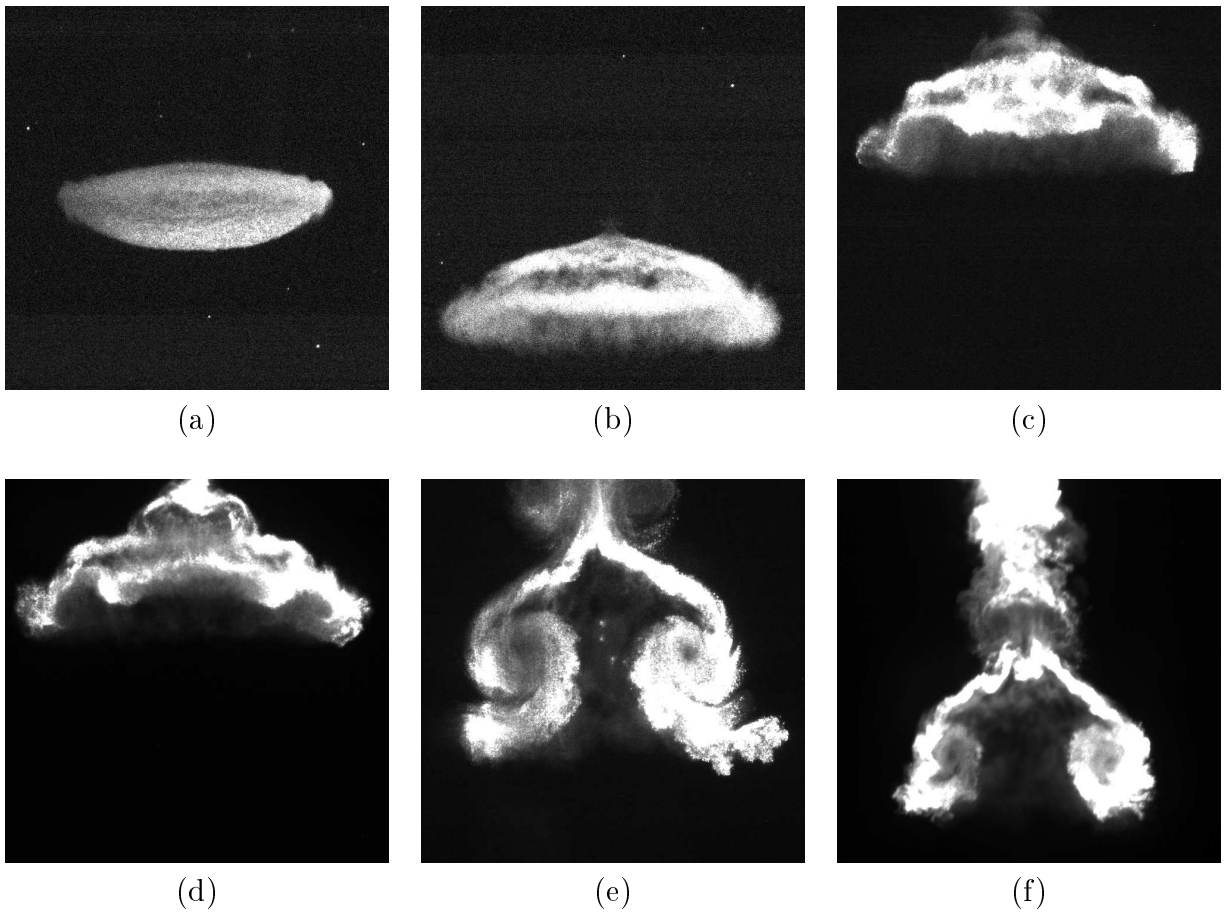

Figure 2: Images of a shock-accelerated argon bubble. $M = 2.88$. (a) 65 μs, (b) 170 μs, (c) 240 μs, (d) 280 μs, (e) 460 μs, (f) 530 μs.

At all shock strengths, the bubble is initially distorted because of pure compression; the vorticity baroclinically deposited on the interface then leads to the formation of a vortex ring seen in cross section at the left and right sides of the bubble; in turn, the vortex ring induces very high strain on the top surface of the bubble, causing it to tilt upwards. The numerical experiments described below have led to the conclusion that the vertical jet visible in the middle of the bubble in Fig.2(f) is caused by an initial accumulation of soap solution at the bottom of the bubble due to gravity. The secondary vortex pair seen at the top of the images in Fig.2(e) and (f) is due to the Kelvin-Helmholtz instability between the vertical jet and the surrounding fluid.

2.1.2 Computational experiments

Extensive computational experiments have been performed using the *Raptor* code made available by Lawrence Livermore National Laboratory. One of our graduate students and one of our scientists have worked very closely from here at UW with Dr. Jeff Greenough of LLNL; and the graduate student has spent twelve summer weeks at LLNL for an internship, also performing computational runs simulating the laboratory experiments.

The overall focus was on identifying the optimum modelling approach that would reproduce the shock tube observations as closely as possible. A wide range of issues was explored, including:

1. 2-D axisymmetric *vs.* full 3-D calculations;
2. massless discontinuous *vs.* massless diffuse *vs.* massive interface;
3. Mach number scaling
4. simulation of small concentration of liquid at the bottom of the bubble.

In all runs, the driven and bubble gases are nitrogen and argon, respectively; a shock travels downwards within the computational domain. Comparison of 2-D and 3-D calculations against the laboratory results shows that, because of 3-D effects induced by azimuthal vortex bending modes, full 3-D calculations (with axial symmetry) are necessary to correctly model the shocked bubble. The calculations also showed that the best way to model the soap film was to introduce a thin layer of fluid at the smallest possible resolution, with density scaled appropriately to capture the total mass of the film material.

Adding a small nonuniformity in the bottom of the bubble film region (simulating fluid accumulation due to gravity) in the calculations' initial conditions, caused the development of a vertical jet in the middle of the bubble of size comparable to that of the jet observed in the laboratory experiments; formation of a secondary vortical structure at the top of the jet (due to the Kelvin-Helmholtz instability) was also observed in both the computational and laboratory experiments.

Figure 3 shows argon volume fraction (left) and total density fields (right) in a vertical plane going through the center of the bubble, at several post-shock times, for a $M = 2.88$ accelerating shock wave. A qualitative comparison to the images shown in Fig.2 demonstrates that the agreement between laboratory and computational experiments is very good.

The evolution of some of the relevant dimensions of the shocked bubble are shown in Fig.4 (a) and (b): It can be seen that Mach number effects are properly scaled by normalizing lengths and times using the initial bubble diameter (D) and the parameter $\tau = D/u_p$, respectively (here u_p is the particle velocity behind the shock in the driven gas).

2.2 New shock tube test section

The test section used in the shock tube experiments in the first two years of the program only contains one pair of windows on opposite, parallel walls; this poses three fundamental limitations to the experiments that can be performed:

1. for a fixed position of the test section along the shock tube, the interface can only be imaged over a very short portion of its trajectory. To observe the interface at a significantly different post-shock time, the shock tube must be reconfigured (at great time expense and personnel cost), placing the test section at a different location along the tube;

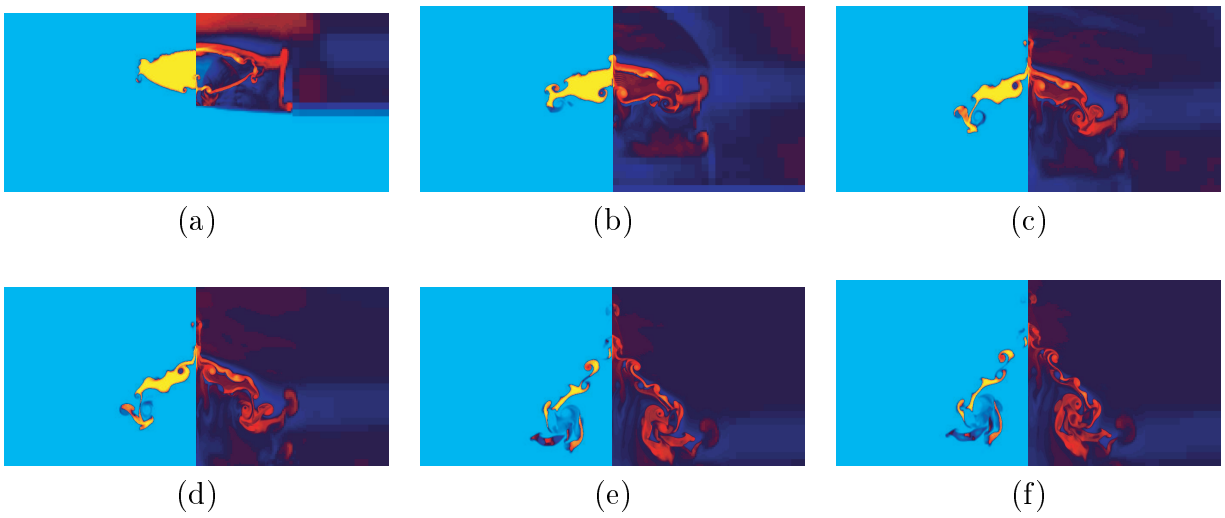

Figure 3: Images of a shock-accelerated argon bubble. $M = 2.88$. (a) 77 μs, (b) 159 μs, (c) 244 μs, (d) 287 μs, (e) 462 μs, (f) 506 μs.

2. with a single optical access, if two images are to be collected during the same experiment, they are necessarily separated by a very short time;

3. the interface (both in the bubble and the 2-D sinusoidal versions) is currently prepared in a shock tube segment (the interface section) which is separated from the test section by at least two flange thicknesses. This makes it impossible to observe the free-falling bubble immediately before the shock wave hits it.

As originally planned, a new test section has been designed and fabricated; the new chamber contains the openings necessary to mount the interface-forming hardware (both for the bubble and the 2-D sinusoid), 12 openings for imaging, and a number of instrumentation ports, thus addressing all three of the limitations posed by the old chamber.

The new test section was fabricated partially in one of the UW-Madison machine shops and partially at outside outfits. As seen in Fig.5, fabrication of the new test section and of all the frames and plugs necessary to hold the quartz windows and to close the openings not used for imaging in a given experiment has been completed. All the necessary quartz windows (for laser entry into the test section and for imaging) have been purchased.

The total cost of the test section (material and fabrication) and of the quartz windows was about $37,000 (including in house personnel cost).

2.3 Richtmyer-Meshkov instability (sinusoidal, 2-D interface)

A technique analogous to that first used by Jeff Jacobs at the University of Arizona has been developed to prepare a 2-D sinusoidal interface without resorting to a membrane or a retractable plate: two different gases flow into the shock tube from its top and bottom and meet head-on forming a stagnation flow that generates a flat interface; two pistons, in opposite shock tube walls, extending about 3 cm both above and below the plane of the stagnation flow, oscillate syncronously extending out of and retracting into the walls, imposing a standing wave onto the interface whose

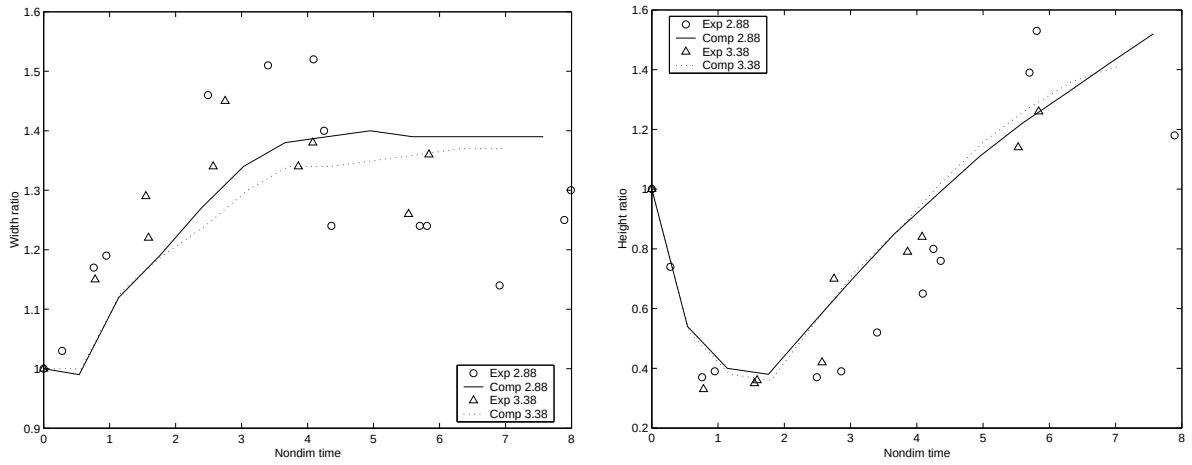

(a) (b)

Figure 4: Comparison of laboratory and computational experiments: (a) bubble width; (b) bubble height. Lengths and time are nondimensionalized using the initial bubble diameter and the quantity $\tau = D/u_p$.

modal content can be adjusted by varying the amplitude and frequency of the pistons' oscillations. The main difference between the present work and Jacobs' is that in that case the entire shock tube is oscillated to impose the perturbation, an approach that would not be suitable for our 9 ton shock tube.

Preliminary experiments have already been performed in the new test section, using shock strengths of $1.3 < M < 1.5$. The gases were N_2 doped with acetone ($\sim 28\%$ volume fraction, correspondng to saturation) coming from the top and SF_6 flowing upward from the bottom of the tube. The interface is visualized once before and twice after interaction with the shock wave by planar laser-induced fluorescence (PLIF) using three separate laser sheet produced by three KrF excimer lasers operating at 248 nm: the first sheet enters the shock tube through the bottom wall while the second and third pulses enter through optical ports in the test section side. A schematic of the system and some sample images are shown in Figs.6 and 7, respectively.

2.4 Rayleigh-Taylor instability

In the first year of funding, a new experiment had been developed for the study of the RT instability, based on the use of a magnetorheological (MR) fluid as one of the two fluids at a perturbed interface. An MR fluid can be "frozen" into any shape by applying a sufficiently large magnetic field; thus, an arbitrary shape can be imposed on the free surface of an MR fluid, and the "frozen" MR fluid can be coupled with a different fluid (*e.g.* water) to form a pair of fluids of different densities separated by a perturbed interface; when the magnetic field is removed, gravity drives the RT instability. Use of an MR fluid thus allows for the preparation of interfaces of any desired shape (in particular, with any superposition of sinusoidal modes) and ensures that the experiment begins with both fluids at rest, without the extra velocity induced by, for example, a retractable plate.

The experiment uses a Plexiglas test section, 6.5 cm wide, 1.27 cm thick, 21.6 cm tall. The MR fluid used is a dispersion of Fe particles (average diameter 4.5 μm) in mineral oil, with a small addition of a surfactant (oleic acid) to prevent coalescence of the Fe particles. The "shaped" MR fluid sits

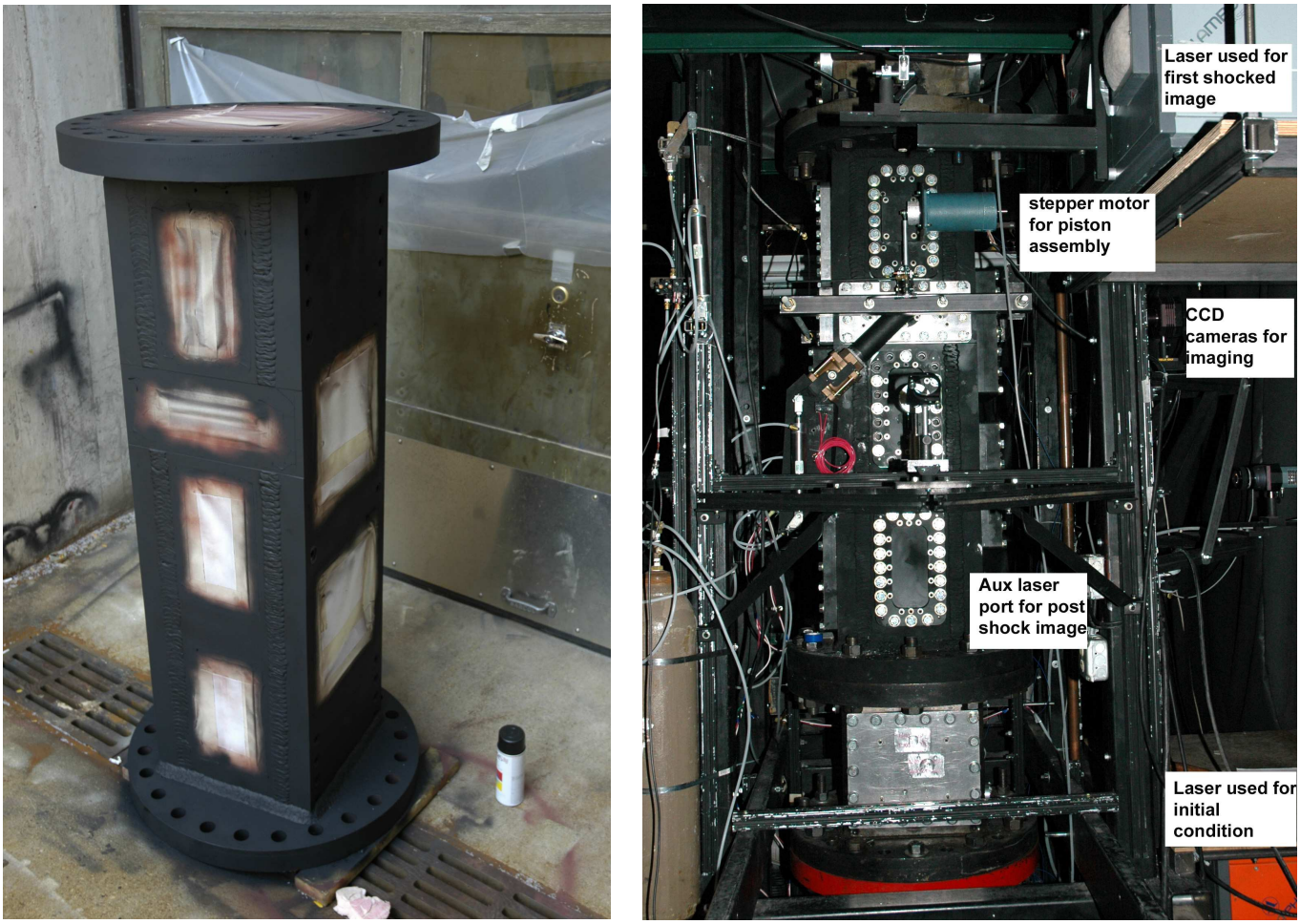

(a) (b)

Figure 5: New shock tube test section: (a) test section (windows openings are covered with paper); (b) test section installed in the shock tube.

on top of water and it is held in place by two sets of permanent magnets (1.5 T each) mounted in two Plexiglas holders. To start the experiment, the magnet holders are retracted away from the test section by two pneumatic cylinders. The interface is illuminated with diffuse, white light and it is imaged using a 512 × 512 pixel CCD camera, operating at 230 fps. Views of the apparatus are shown in Figs.8(a) and (b).

The density of the MR fluid, and consequently the Atwood number at the interface, can be altered by changing the volume fraction of the Fe in the dispersion, ϕ. Experiments have been performed using Fe volume fractions ϕ =15%, ϕ =20% and ϕ =30%, corresponding to Atwood numbers A =0.28, A =0.35 and A =0.47, respectively; and using two different initial interface shapes: a single-mode sinusoid, with η =3.2 mm and λ =21.2 mm, and a two-mode superposition with η_1 =3.2 mm, λ_1 =21.2 mm and η_2 =1.9 mm, λ_2 =12.7 mm.

Sample images for a two-mode experiment with A=0.35 are shown in Fig.9.

Several image processing algorithms have been developed and implemented using the Matlab programming environment to automate the extraction of relevant geometrical data from each image.

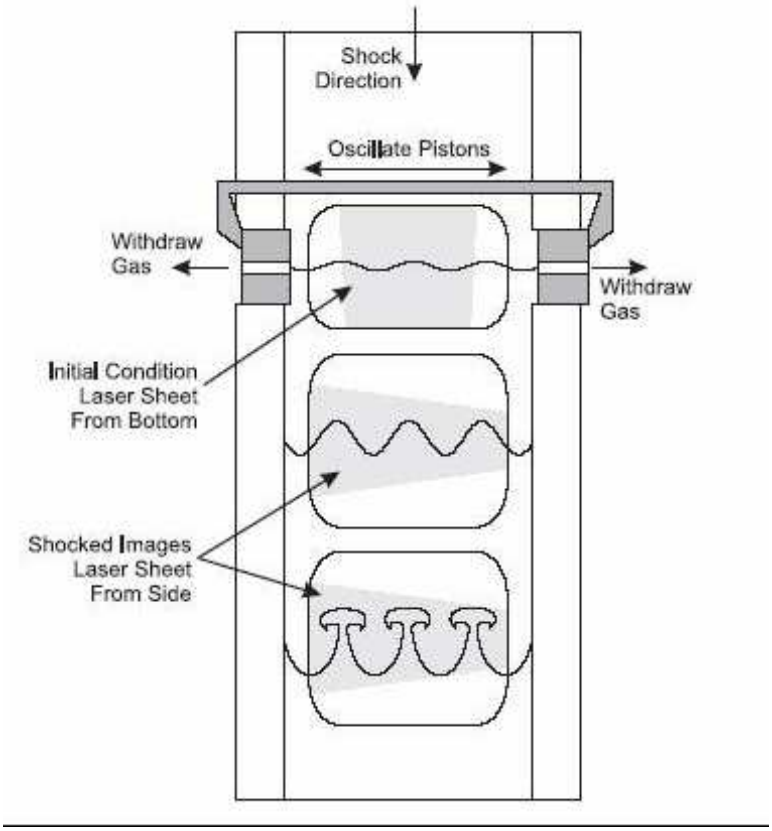

Figure 6: Schematic of 2-D RMI experimental setup.

Sample amplitude data for a 2-modes (3 and 5) interface are presented in Fig.10.

3 Work for the current year of funding

Extensive shock tube experiments will be performed using the new test section. The free-falling bubble will be studied further, with an effort to identify the existence of a particular value of the incident shock strength at which compressibility effects are no longer negligible. Extensive PLIF experiments with the 2-D sinusoidal interface will be performed.

Rayleigh-Taylor experiments based on the use of MR fluids will be pursued further with particular emphasis on material selection for the fluid pair. By judiciously adjusting the diluent, the iron concentration and the other fluid at the interface, the Atwood and Reynolds number and the fluid miscibility will be pushed towards their most interesting values.

Numerical experimentation will also continue, both here at UW and, hopefully, with one of our graduate student once again in residence at LLNL for a period of time.

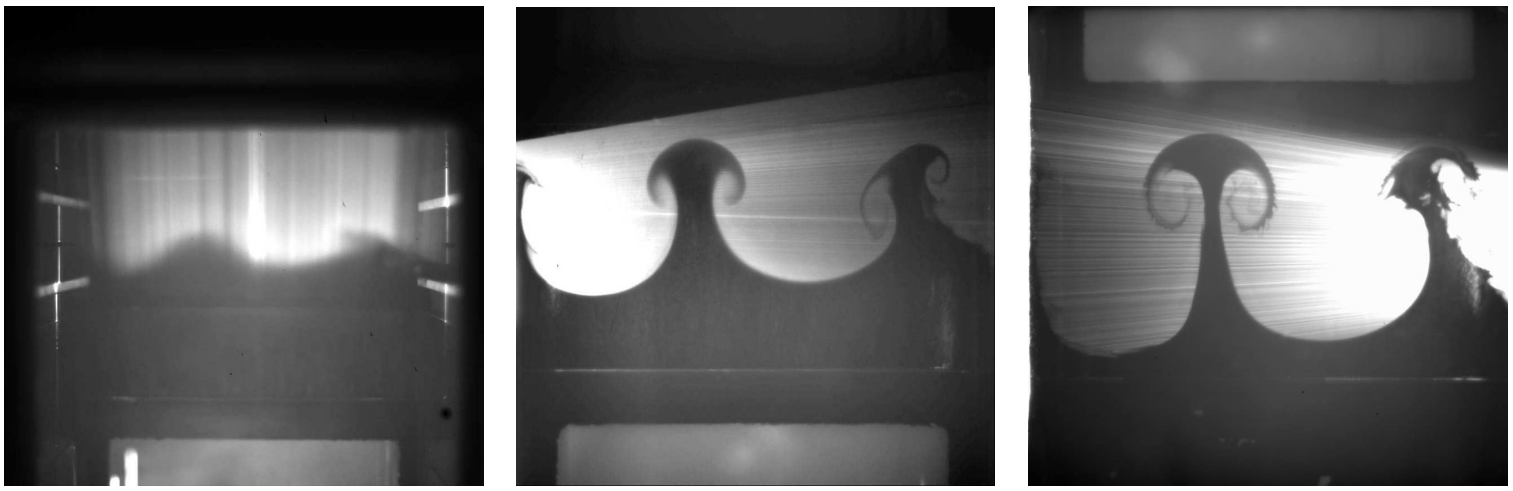

(a) (b) (c)

Figure 7: Preliminary 2-D RM experiments. $M = 1.41$. (a) $t = 0$; (b) $t = 3.36$ ms; (c) $t = 5.83$ ms.

4 Publications and presentations

Our work was presented at the 24th International Symposium on Shock Waves (Beijing, July 2004) and at the 9th International Workshop on the Physics of Compressible Turbulent Mixing (Cambridge, England, July 2004). More recent progress will be presented at the meetings of the APS divisions of Plasma Physics and Fluid Dynamics, in October and November 2004, respectively.

An article was published: P.B. Puranik, J.G. Oakley, M.H. Anderson, R. Bonazza., "Experimental study of the Richtmyer-Meshkov instability induced by a Mach 3 shock wave", *Shock Waves*, **13**, 2004. A letter has been submitted to Physics of Fluids.

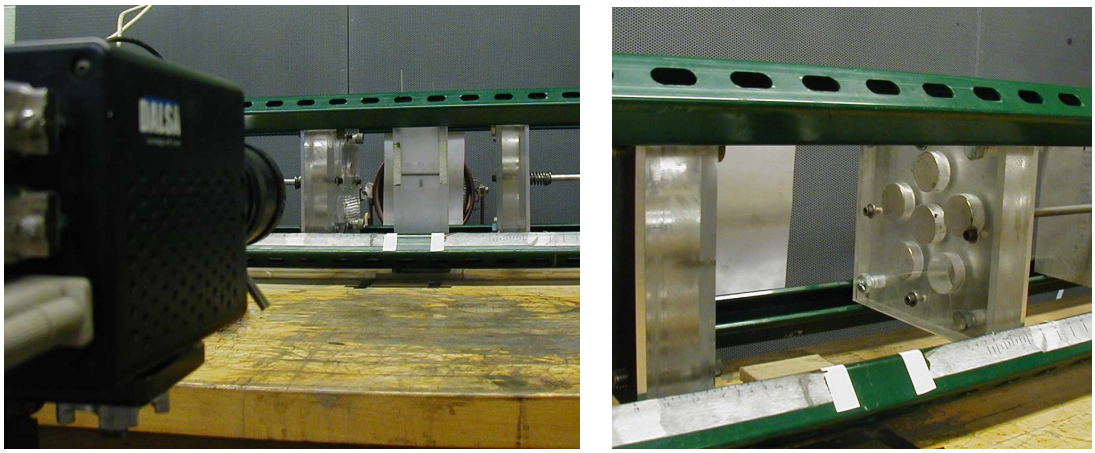

(a) (b)

Figure 8: Views of setup for RT experiments: (a) imaging CCD, test section and magnet magazines; (b) detail of magnet magazine.

5 Personnel

Faculty and staff involved in and supported by the program include:

Prof. Riccardo Bonazza, Associate Professor, Dept. Engineering Physics; supported for 2.7 months.
Prof. Leslie Smith, Full Professor, Depts. Mathematics and Engineering Physics; supported for 1.0 month.

Dr. Mark Anderson, Associate Scientist, Dept. Engineering Physics; supported for 7.1 months.
Dr. Jason Oakley, Assistant Scientist, Dept. Engineering Physics; supported for 10 months.

Mr. Paul Brooks, Instrumentation Specialist, Dept. Engineering Physics; supported for 4.5 months.

Graduate students supported by and fully involved in the program in the past year include:

Mr. Brad Motl (USA; pursuing a Ph.D. degree); supported for 12 months.
Mr. John Niederhaus (USA; pursuing a Ph.D. degree); supported for 12 months.
Mr. Devesh Ranjan (India; pursuing a Ph.D. degree); supported for 12 months

About 6 undergraduate students were also involved in and supported by the program at various levels and for different lengths of time.

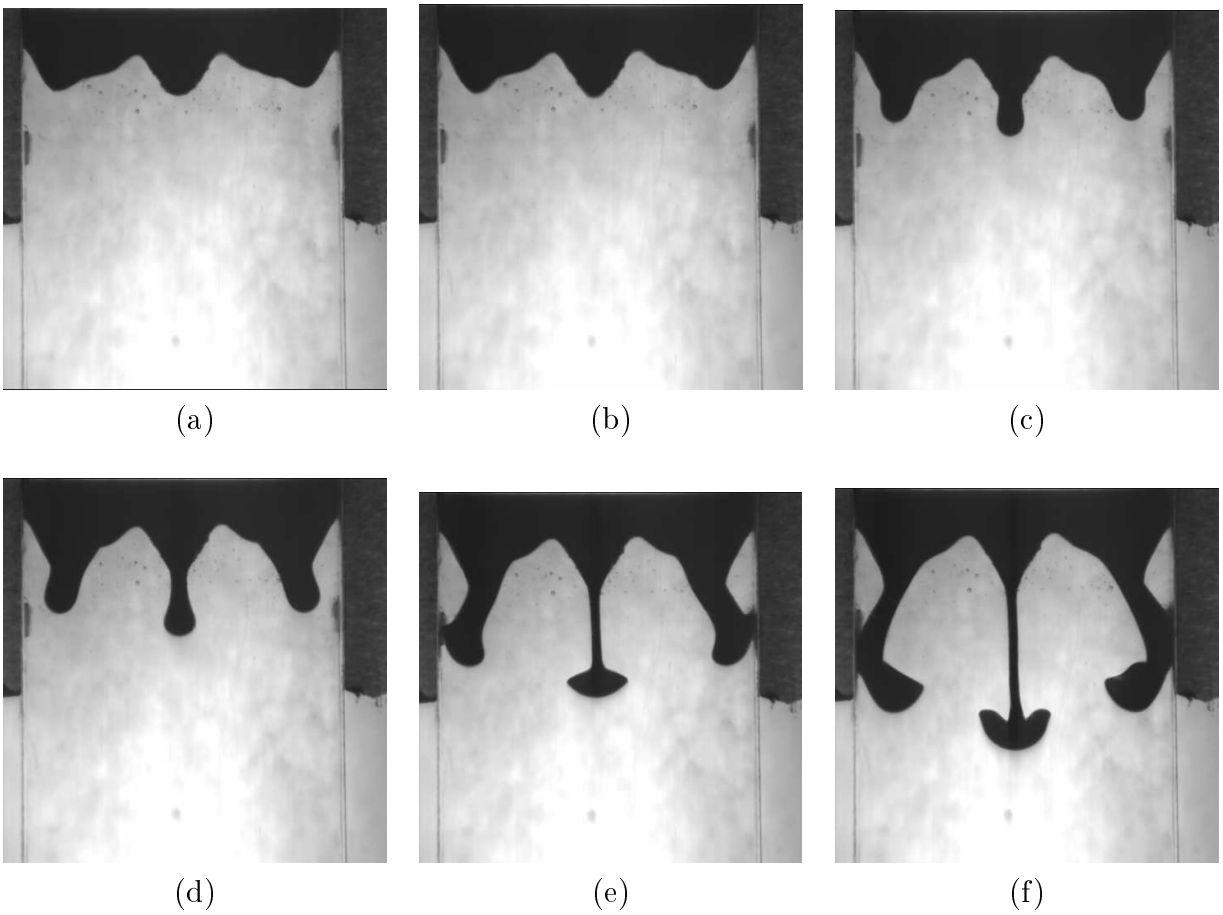

Figure 9: Images of a multimode MR fluid/water interface. $\phi = 20\%$, $A = 0.35$. (a) 0 s, (b) 92 ms, (c) 168 ms, (d) 206 ms, (e) 264 ms, (f) 321 ms.

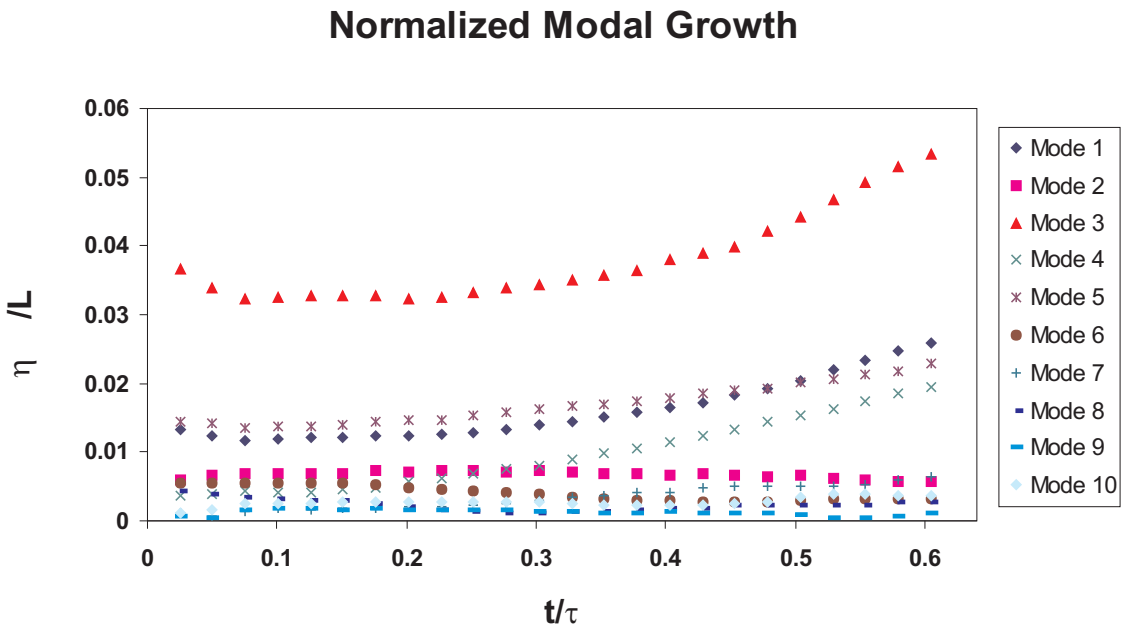

Figure 10: Modal growth on a 2-modes (3 and 5) interface.